Journal of Marine Research, 47, 153–168, 1989

Longitudinal dispersion of suspended particles in oscillatory currents

by Hidekazu Yasuda[1]

ABSTRACT

This study has investigated theoretically longitudinal dispersion of suspended fine particles with settling velocity and revealed the dispersing behavior from the initial to the stationary stages in tidal oscillatory currents. A Stokes layer of the oscillatory current plays a remarkably significant role on dispersion of settling particles when the mixing time in cross-section is larger than the period of tidal oscillation. When the settling velocity exceeds a certain value, however, the dispersion coefficient of particles decreases with increasing settling velocity. In an oscillatory current with linear profile, settling velocity of dispersing particles decreases the value of the dispersion coefficient all over the values of the settling velocity.

1. Introduction

Longitudinal dispersion of matter due to the shear effect, which is produced by the combined action of current shear and mixing in the cross-sectional plane, has been presented by Taylor (1953, 1954), and has in sequence examined as the third mechanism of mixing process next to molecular and turbulent diffusions by many researchers (reviewed in Fischer, 1976 and Fischer *et al.*, 1979). Longitudinal dispersion in oscillatory currents has been analyzed by Bowden (1965), Okubo (1967), Holley *et al.* (1970), Fukuoka (1973), Smith (1982, 1983), Yasuda (1982), Young *et al.* (1982) and so on, to understand the mass transport mechanism in coastal seas. Usual studies using a simplified current profile have concluded that longitudinal dispersion due to oscillatory currents is negligibly small when the mixing time in cross-sectional plane is much larger than the tidal period. An oscillatory current generally forms a Stokes layer, the thickness of which is determined by the viscosity and the tidal frequency (Lamb, 1932). Yasuda (1982, 1988) has shown that a Stokes layer produces some dispersion effect and further that the layer could play a significant role on the matter dispersion in tidal waters especially at the initial stage in the case of a point-source. A large dispersion coefficient during the initial stage is caused by the fact that the dispersing matter exists inside or near the Stokes layer. Suspended particles with settling velocity are often observed near the sea floor, and thus such

1. Government Industrial Research Institute, Chugoku 2-2-2, Hiro-Suehiro, Kure-city, Hiroshima 737-01, Japan.

particles may be dispersed effectively in horizontal direction by the Stokes layer. From these, this study will analyze longitudinal dispersion of settling fine particles in oscillatory currents as an advanced investigation of the previous works (Yasuda, 1982 and 1988).

Works on longitudinal dispersion of settling particles, of which there are only a few, have been done by Sumer (1974, 1977), Wilson and Okubo (1978), Awaya and Fujisaki (1981) and so on. Sumer and Awaya and Fujisaki analyzed it at the stationary stage assuming turbulent steady flow, while Wilson and Okubo examined it in an oscillatory current with linear profile and suggested that the vertical advection could weaken the longitudinally dispersing effect. This study will analyze dispersion process from the initial to the stationary stage in an oscillatory current with a Stokes layer and will show that the settling velocity can induce the longitudinal dispersion of particles with effect in tidal basin.

2. Analysis of the advection-diffusion equation in a two-dimensional basin

In order to understand the nature of longitudinal dispersion of suspended particles in tidal basins, we introduce a simplified longitudinal vertical plane model with two-dimensions (x-z plane) similar to the previous reports (Yasuda, 1982, 1984, 1988). The water depth and the current velocity are assumed to be uniform in the longitudinal (x-axis) direction. The longitudinal mixing due to the horizontal diffusivity is neglected because it is independent of the shear effect analyzed in this study. The concentration of the suspended settling particles, $S(x, z, t)$, is governed by the following advection-diffusion equation;

$$\frac{\partial S}{\partial t} + u(z, t)\frac{\partial S}{\partial x} + w\frac{\partial S}{\partial z} = k_z\frac{\partial^2 S}{\partial z^2} \tag{1}$$

where $u(z, t)$ is the longitudinal current, w and k_z are the settling velocity of particles and the vertical diffusivity, respectively, which are assumed constant. If the diffusing matter is perfectly passive, the third term can be neglected such as in the usual analyses of the dispersion. The settling velocity w gives the following boundary condition at the bottom and the water surface;

$$wS - k_z\frac{\partial S}{\partial z} = 0 \qquad \text{at} \begin{cases} z = 0 \text{ (the bottom)} \\ z = H \text{ (the water surface)} \end{cases} \tag{2}$$

The above boundary condition is derived from the conservation of $S(x, z, t)$ in the vertical and can be expressed when w is not so large as that of silt or sand. It seems to be hard for such heavy particles to rise up again after settling on the bottom. The boundary condition in the x-direction is implicitly given as $S = 0$ at $x \to \pm\infty$. The initial condition is given as an instantaneous point-source at $x = 0$ and $z = z_0$

$$S(x, z; 0) = S_0\delta(x)\delta(z - z_0). \tag{3}$$

The longitudinal dispersion will be analyzed using the Aris's moment method (1956) similar to the previous reports (Yasuda, 1982, 1984, 1988). The equation governing the p-th order moment $M_p(z, t)$, which is defined as $\int_{-\infty}^{\infty} x^p S(x, z, t)dx$, is

$$\frac{\partial M_p}{\partial t} + w\frac{\partial M_p}{\partial z} - k_z\frac{\partial^2 M_p}{\partial z^2} = puM_{p-1} \qquad (p \geq 1). \tag{4}$$

The boundary condition for M_p at the bottom and the surface is written as

$$wM_p - k_z\frac{\partial M_p}{\partial z} = 0. \tag{5}$$

The zeroth-order moment $M_0(z, t)$ is governed by the following homogeneous parabolic partial differential equation:

$$\frac{\partial M_0}{\partial t} + w\frac{\partial M_0}{\partial z} = k_z\frac{\partial^2 M_0}{\partial z^2}. \tag{6}$$

The boundary condition is the same as (5).

The zeroth-order moment at the stationary stage, $M_{0_\infty}(z)$, can be obtained from elimination of the first term of (6);

$$M_{0_\infty}(z) = \frac{S_0}{H}\frac{k_z}{w}\frac{e^{w/k_z H}}{e^{w/k_z H} - 1}. \tag{7}$$

The coefficient S_0/H contained in every moment is omitted in the following by regarding it as unity. The principal solution of (6) can be obtained as (e.g. Farlow, 1982)

$$\begin{aligned} G_0(z, t, \xi, \tau) = {} & \frac{\omega}{e^{\omega} - 1} e^{\omega(z/H)} + \frac{1}{2}\sum_{n=1}^{\infty}\frac{e^{K_n(\tau - t)}}{M_n^2}\{\omega e^{(\omega/2)(z/H)}\sin p_n z \\ & + 2n\pi e^{(\omega/2)(z/H)}\cos p_n z\}\{\omega e^{-(\omega/2)(\xi/H)}\sin p_n\xi + 2n\pi e^{-(\omega/2)(\xi/H)}\cos p_n\xi\} \end{aligned} \tag{8}$$

where $\omega = wH/k_z$, $M_n^2 = (\omega/2)^2 + (n\pi)^2$, $K_n = M_n^2 k_z/H^2 = M_n^2/T_c$ and $p_n = n\pi/H$. Characters ω and T_c are defined in the Appendix. From Eq. (8), $M_0(z, t)$ is

$$M_0(z, t) = \frac{\omega}{e^{\omega} - 1} e^{\omega(z/H)} + \frac{1}{2}\sum_{n=1}^{\infty}\frac{e^{-K_n t}}{M_n^2}\{\alpha_{1n}(z) + \alpha_{2n}(z)\}F_n(z_0) \tag{9}$$

where $\alpha_{1n}(z) = \omega e^{(\omega/2)(z/H)}\sin p_n z$, $\alpha_{2n}(z) = 2n\pi e^{(\omega/2)(z/H)}\cos p_n z$ and $F_n(z_0) = \omega e^{-(\omega/2)(z_0/H)}\sin p_n z_0 + 2n\pi e^{-(\omega/2)(z_0/H)}\cos p_n z_0$. The solution (9) has already been shown in Wilson and Okubo (1978).

The formal solution of (4), which is a nonhomogeneous parabolic type equation, is

$$M_p(z, t) = p\int_0^H\int_0^t G_0(z, t, \xi, \tau)u(\xi, \tau)M_{p-1}(\xi, \tau)d\tau d\xi. \tag{10}$$

This shows that each moment can be subsequently solved by the knowledge of $M_0(z, t)$. The vertically averaged moment is given through integrating (4) over $0 \leqq z \leqq H$ and $0 \leqq t \leqq t$

$$\overline{M}_p(t) = p\int_0^H \int_0^t u(\xi, \tau)M_{p-1}(\xi, \tau)\, d\tau d\xi. \tag{11}$$

The variance giving the degree of dispersion by mixing is defined as (Yasuda, 1988)

$$\overline{\sigma_x^2}(t) = \overline{\sigma_x^2(z, t)M_0(z, t)} = \overline{M}_2(t) - \left\{\frac{\overline{M_1(z, t)^2}}{\overline{M_0(z, t)}}\right\}. \tag{12}$$

The usual variance introduced from the vertically averaged matter concentration is written as

$$\begin{aligned}\overline{\sigma_x^2}^*(t) &= \int_{-\infty}^{\infty} \{x - \overline{M}_1(t)\}^2 \overline{S}(x, t)\, dx \\ &= \overline{M}_2(t) - \overline{M}_1(t)^2\end{aligned} \tag{13}$$

where overbar denotes the operation of vertical average. The longitudinal dispersion coefficients are given from the respective variances as

$$\overline{D}(t) = \frac{1}{2}\frac{d\overline{\sigma_x^2}}{dt}, \quad \overline{D}^*(t) = \frac{1}{2}\frac{d\overline{\sigma_x^2}^*}{dt}. \tag{14), (15}$$

An oscillatory current with a Stokes layer has been given by Lamb (1932) as

$$u(z, t) = U[(1 - e^{-\beta z}\cos\beta z)\sin\sigma t + e^{-\beta z}\sin\beta z\cos\sigma t] \tag{16}$$

where σ is the frequency of the oscillatory current and $\beta = \sqrt{\sigma/2\nu_z}$, the reciprocal of which is representative of the characteristic thickness of the Stokes layer. ν_z is the vertical viscosity assumed constant.

The tidally averaged dispersion coefficient at the stationary stage can be obtained using the second-order moment with tidal variation eliminated at large t as $\exp(-K_n t)$ disappears:

$$\overline{D}_\infty = \frac{U^2}{\sigma}\frac{\omega}{2(e^\omega - 1)}\sum_{n=1}^{\infty}\frac{K_n}{K_n^2 + \sigma^2}\frac{P_n^2 + Q_n^2}{M_n^2} \tag{17}$$

where $P_n = \int_0^H \alpha_{1n}(\xi)\eta_1(\xi)d\xi + \int_0^H \alpha_{2n}(\xi)\eta_1(\xi)d\xi$, $Q_n = \int_0^H \alpha_{1n}(\xi)\eta_2(\xi)\, d\xi + \int_0^H \alpha_{2n}(\xi)\eta_2(\xi)d\xi$. $\eta_1(\xi)$ and $\eta_2(\xi)$ correspond to $1 - e^{-\beta\xi}\cos\beta\xi$ and $e^{-\beta\xi}\sin\beta\xi$, respectively, which express the vertical profile of the current in this study.

3. Solution curves on the longitudinal dispersion of settling particles

Although longitudinal dispersion of passive matter, corresponding to the case of $\omega = 0$, has been examined by many researchers, the behavior of longitudinal dispersion of

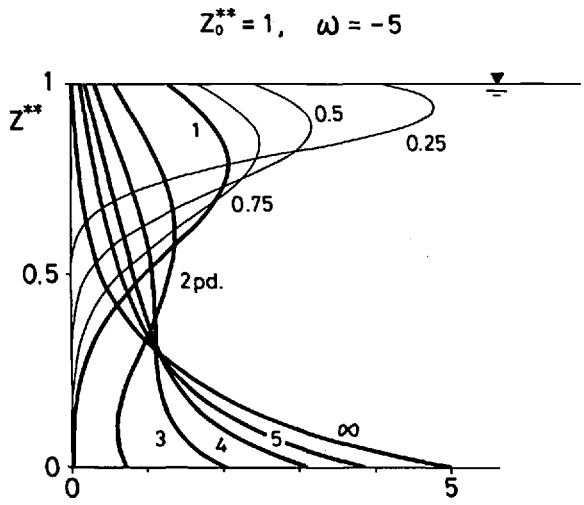

Figure 1. Variation with time of the vertical profile of $M_0(z, t)$. The release point is at the water surface ($z_0^{**} = 1$), and the nondimensionalized vertical advection ($\omega = wH/k_z$) is -5. Numerals in this figure represent the elapsed time representing the tidal period. One tidal period corresponds to $T_c/31.83$.

settling particles in oscillatory currents has not yet been studied. In order to understand the nature of longitudinal dispersion of such particles, I will show detailed behavior of dispersing particles first. The following is the case where H^* ($= \beta H$) = 10, ω ($= wH/k_z$) = -5 and z_0^{**} ($= z_0/H$) = 1. The equation $z_0^{**} = 1$ means that the source of the dispersing particles is given instantaneously at the water surface. These numerical values, for example, correspond to the case that the water depth is about 12 m and the settling velocity is about 0.004 cm/sec (15 cm/hr) if $k_z = \nu_z = 1$ cm^2/sec. The relation $k_z = \nu_z$ is assumed in figures of this study so as not to be more complicated by an unknown parameter, k_z/ν_z. Figure 1 shows the variation with time of the vertical profile of the zeroth-order moment. In this case, T_r (= characteristic time of vertical mixing T_c/tidal period T) is nearly 31.8 and one tidal period corresponds to 0.0314 T_c (see Appendix). The profile at the 5th tidal period looks to reach that at the stationary stage, further the profile at $t = 0.5\ T_c$ (about the 15th tidal period) almost corresponds to the stationary one (denoted by ∞).

Figure 2 shows the vertical profiles of the normalized first-order moment during the initial first period and the stationary stage period. For comparison, those in the case of a line source ($w = 0$) and water particle displacement (corresponding to the case of $k_z = 0$ and $w = 0$) are drawn in this figure.

Under the situation of Figures 1 and 2, the variance increases as time proceeds and the increasing rates induce the longitudinal dispersion coefficients as shown in Figure 3. Solid and broken lines express the dispersion coefficients given by Eqs. (14) and (15), respectively. The dispersing effect has not yet been observed during the

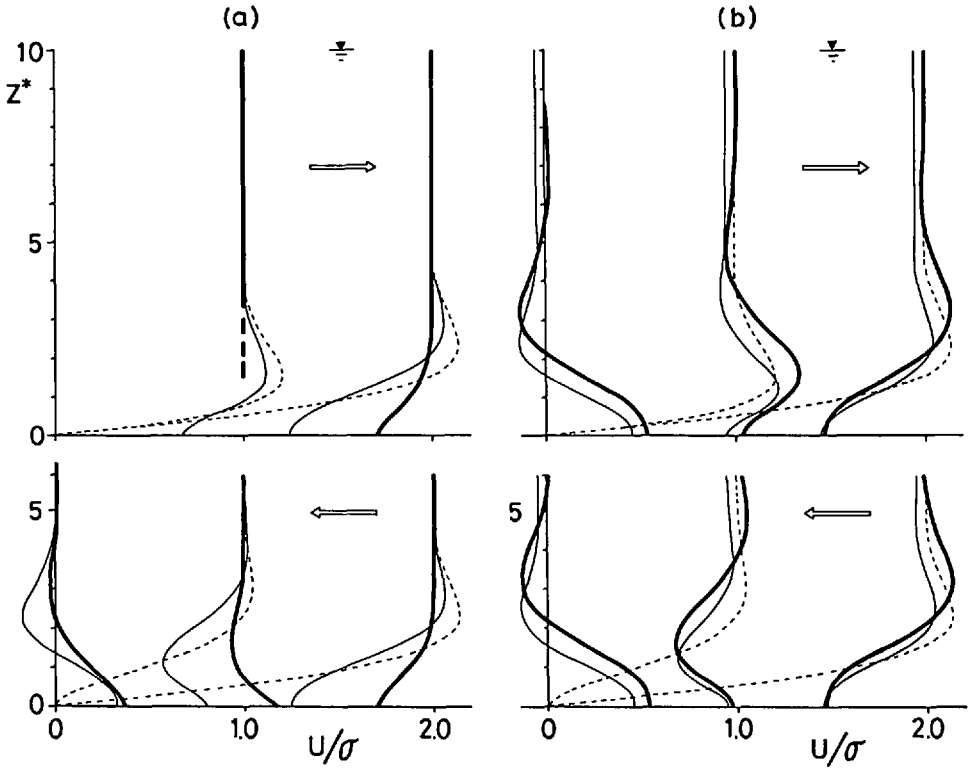

Figure 2. Vertical profiles of $M_1(z, t)/M_0(z, t)$. Each group of profiles is drawn at every quarter of one tidal oscillation. (a) shows the initial one tidal period and (b) one tidal period at the stationary stage. The solid thick and thin lines correspond to the cases of a point-source ($z_0^{**} = 1, \omega = -5$) and a line-source ($\omega = 0$) respectively. The broken line corresponds to the water particles displacement obtained from $\int_0^t u(z, t)dt$.

initial first tidal period when much of the particles are outside the Stokes layer, while the longitudinal dispersion gradually appears as the particles enter inside the Stokes layer (see Fig. 1).

Figure 4 is the tidally averaged dispersion coefficients and the values denoted by the equation $z_0^{**} = 1$ corresponds to Figure 3. The solid and broken lines give the same expression as those of Figure 3. In addition, the values denoted by $z_0^{**} = 0$ is the dispersion coefficient in the case where a point-source is released at the bottom. The variation of $M_0(z, t)$ in this case is drawn as Figure 5. At the stationary stage, both M_0 and the dispersion coefficient are independent of the position of the release point. This averaged dispersion coefficient at the stationary stage is about $1.93 \times 10^{-2}\, U^2/\sigma$ while the coefficient was given as $0.62 \times 10^{-2}\, U^2/\sigma$ in the case of passive (neutrally buoyant) matter ($\omega = 0$; Yasuda, 1982, 1988).

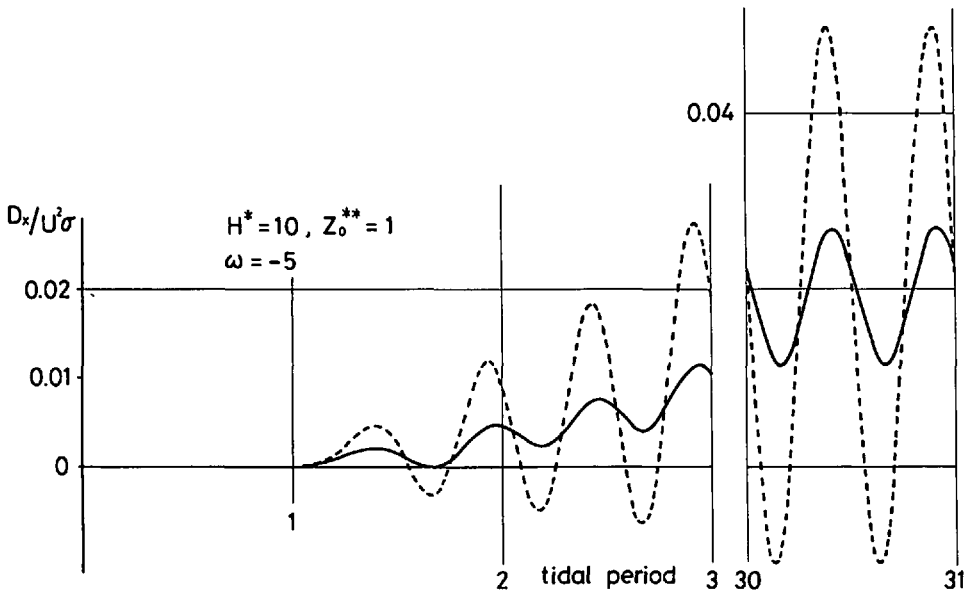

Figure 3. Variations of the dispersion coefficients with time ($H^* = 10$, $z_0^{**} = 1$ and $\omega = -5$). Solid and broken lines represent the values by (14) and (15), respectively.

The dispersion coefficients at the stationary stage in the oscillatory current with a Stokes layer are given by (17) and are drawn as a function of the settling velocity at each H^* as Figure 6. The nondimensionalized settling velocity, ω^*, of the abscissa is introduced to express the dependence on the settling velocity more clearly. This nondimensional velocity is related to the former velocity by $\omega = H^* \cdot \omega^*$ (see the Appendix). The former velocity $\omega = -5$ at $H^* = 10$ of Figures 3 and 4 corresponds to $\omega^* = -0.5$ of Figure 6. Though this figure shows that the coefficient at $\omega^* = -0.5$ of $H^* = 10 (\omega = -5)$ is about three times larger than that at $\omega^* = 0$ as described in the above, the dispersion coefficient does not necessarily become larger with the increment of the settling velocity and has a maximum at $\omega^* = -1$ in every case. When the settling velocity is very large ($\omega^* < -1$), the particles are in a bottom layer which is thinner than the Stokes layer and thus are not affected by the shear of the Stokes layer. As the upward velocity ($\omega^* > 0$, denoting light particles compared to the water density) increases, the dispersion coefficient decreases because much of the particles are outside the Stokes layer and the particles are less affected by the shear of the Stokes layer. The vertical profiles of $M_{0\_}(z)$ are drawn in Figure 7 to show correspondence between the dispersion coefficient and the vertical distribution of settling particles. Numerals in this figure denote ω not ω^*. When particles have upward velocity, they are in the upper layer and the distribution is symmetrical with respect to the line $z^{**} = 0.5$ ($z = 0.5\,H$).

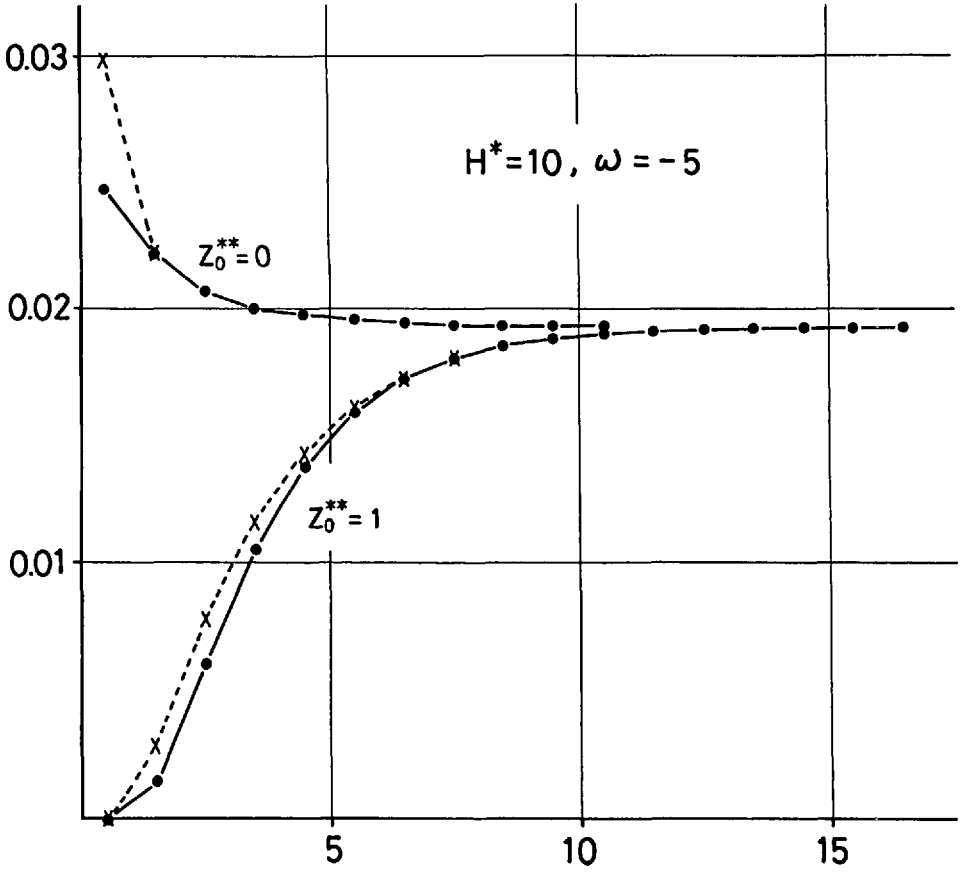

Figure 4. Variations of the tidally averaged dispersion coefficient with time.

Figure 8 shows the temporal variations of the tidally averaged dispersion coefficient in the case of $\omega = -10$ where the stationary dispersion coefficient has maximum (Fig. 6). The larger settling velocity causes the dispersion effect and allows the dispersion coefficient to reach the stationary value at the earlier stage compared to Figure 4.

The solution in the line-source case can be obtained by substituting $\int_0^H F_n(z_0)dz_0/H$ for $F_n(z_0)$ appearing in (9) and so on. Figure 9 shows the variation of the vertical profile of $M_0(z, t)$ from the line-source in the case of $H^* = 10$ and $\omega = -5$. A thick line in Figure 10 is the variation of the dispersion coefficient with time in this case. Both figures show that the dispersion coefficient becomes larger as particles settle. A thin line in Figure 10 shows the dispersion coefficient of neutrally buoyant matter ($\omega = 0$) which has been investigated in Yasuda (1982).

Many analyses of the longitudinal dispersion have been made using simplified

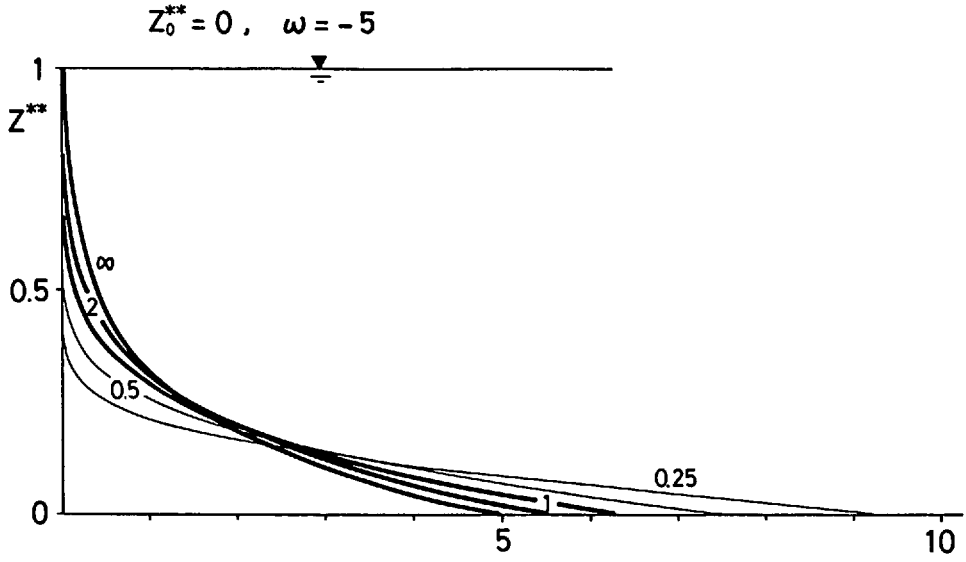

Figure 5. Variation with time of the vertical profiles of $M_0(z, t)$ in the case where the point-source is released at the bottom ($z_0^{**} = 0$).

current profiles. Wilson and Okubo (1978) concluded through the analysis of dispersion of matter with vertical advection in a current with linear profile that vertical advection, w, might make the dispersing effect at the stationary stage smaller under the condition of $T_r \gg 1$. The dispersion in an oscillatory current with linear profile can be examined using the following current instead of (16),

$$u(z, t) = U\frac{z}{H}\sin \sigma t. \tag{18}$$

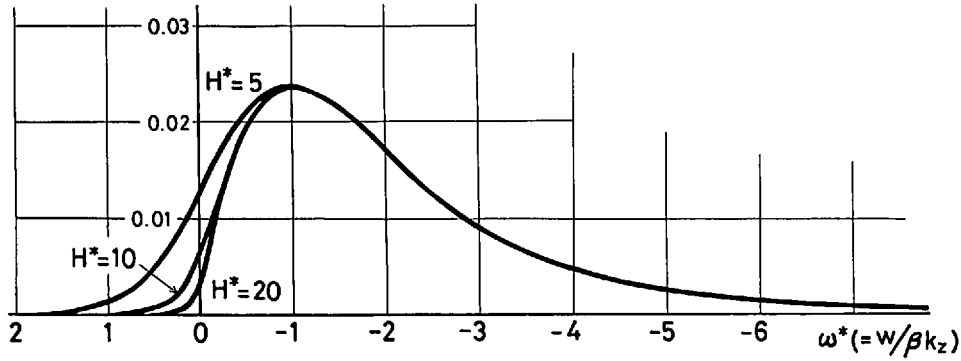

Figure 6. Variations with $\omega^*(=w/\beta k_z)$ of the averaged dispersion coefficient at the stationary stage in currents with the Stokes layer.

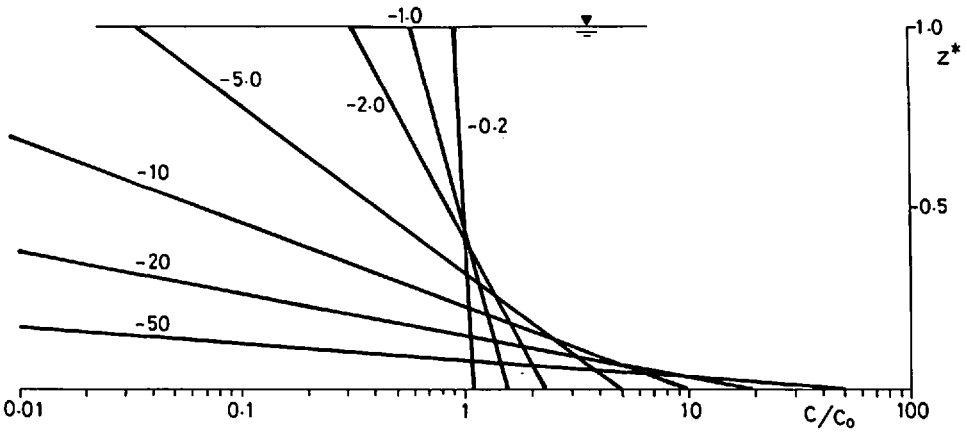

Figure 7. Vertical profiles of the zeroth-order moment at the stationary stage. Numerals in the figure denote the value of $\omega(=wH/k_z)$.

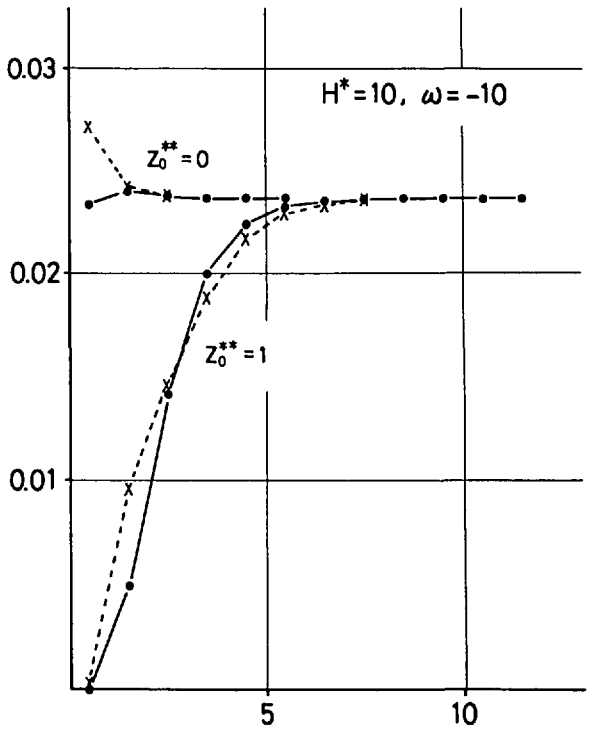

Figure 8. The tidally averaged dispersion coefficient ($H^* = 10$ and $\omega = -10$).

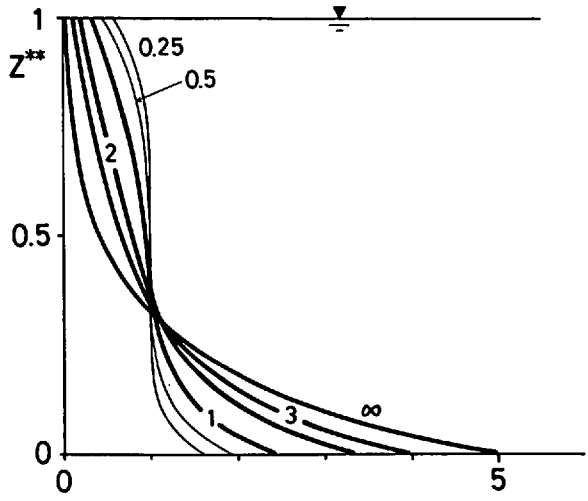

Figure 9. Variation with time of $M_0(z, t)$ in the case of a line-source ($H^* = 10$ and $\omega = -5$).

The dispersion coefficient with the periodical variation eliminated at the stationary stage in the linear profile current can be given as

$$\overline{D}_\infty = \frac{U^2}{\sigma} \frac{\omega}{2(e^\omega - 1)} \sum_{n=1}^{\infty} \frac{K_n}{K_n^2 + \sigma^2} \frac{R_n^2}{M_n^2} \tag{19}$$

where $R_n = \int_0^H f(\xi)\alpha_{1n}(\xi)d\xi + \int_0^H f(\xi)\alpha_{2n}(\xi)d\xi$ and $f(\xi) = \xi/H$ giving the vertical profile.

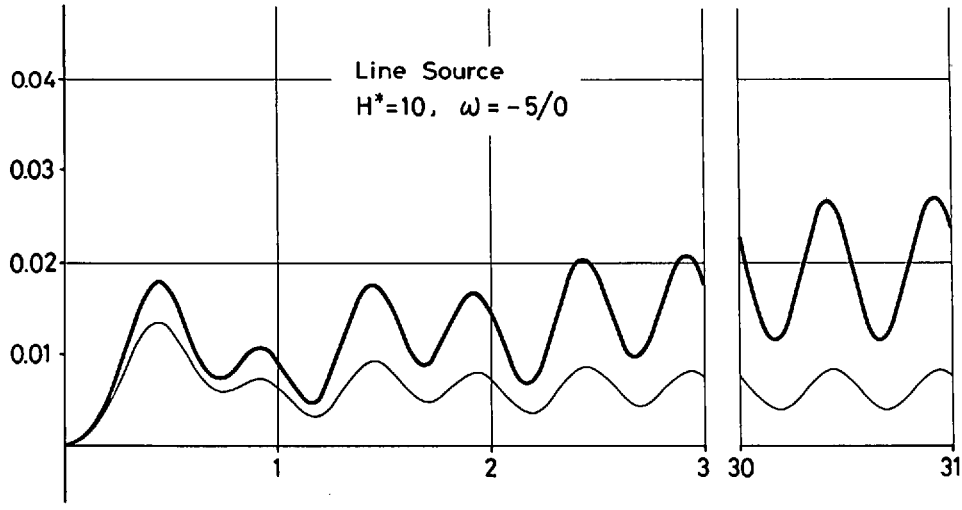

Figure 10. The dispersion coefficients from a line-source ($H^* = 10$). Thick and thin lines correspond to the cases of $\omega = -5$ and $\omega = 0$, respectively.

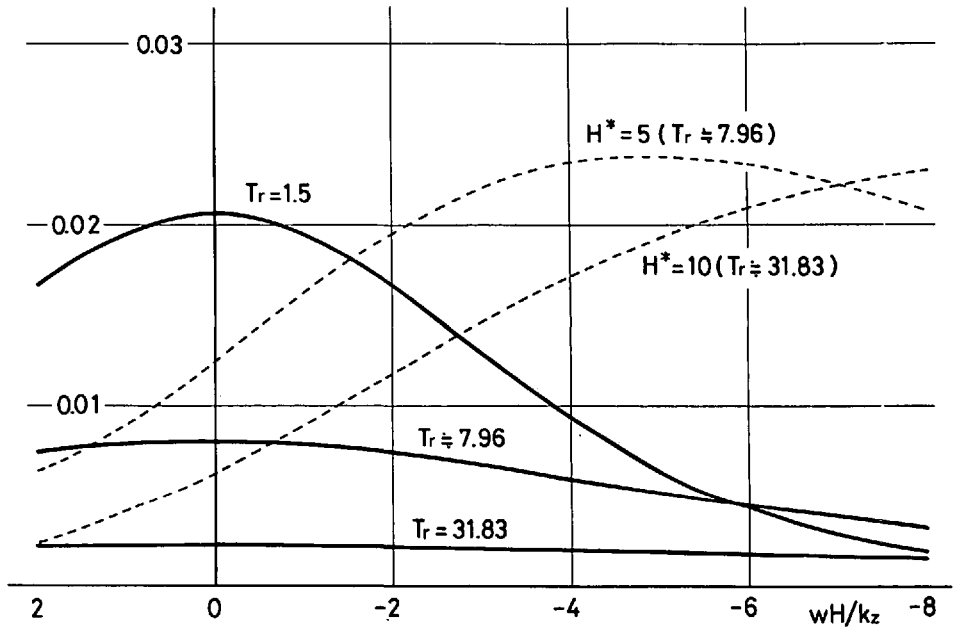

Figure 11. Variations with ω of the dispersion coefficients at the stationary stage in linear profile currents at each T_r (solid lines) and those in currents with Stokes layer (broken lines).

Figure 11 is the variations with $\omega(= wH/k_z)$ of the stationary dispersion coefficient in the linear profile current (drawn by solid lines). The dispersion coefficient at $T_r = 1.5$ gives the maximum value in the case of no settling velocity. $T_r = 7.96$ and 31.83 are respectively given in the basins with $H^* = 5$ and 10 (currents with the Stokes layer) assuming that ν_z equals to k_z (see the Appendix). The broken lines show the dispersion coefficient due to the current with the Stokes layer, which are the same as Figure 6. Both solid and broken lines represent difference of the dependence of the dispersion coefficient on the current profile. The solid lines show that the dispersion coefficients due to the linear profile current are symmetric with respect to $\omega = 0$ and decrease as the absolute value of ω increases regardless of the sign of ω. Figure 12 shows the time-dependence of the tidally averaged dispersion coefficients in both cases of settling velocity. Solid and broken lines correspond to those in Figure 3 etc. The difference between the two cases of settling velocity results from the behavior of $M_0(z, t)$. The reason why the dispersion coefficient in the case with settling velocity is smaller than that in the case with no settling velocity is considered as follows: dispersing particles with settling velocity are partially distributed near the bottom and they are influenced by the current shear less effectively than particles with no settling velocity which are uniformly distributed in the whole depth at the stationary stage. This is physically the

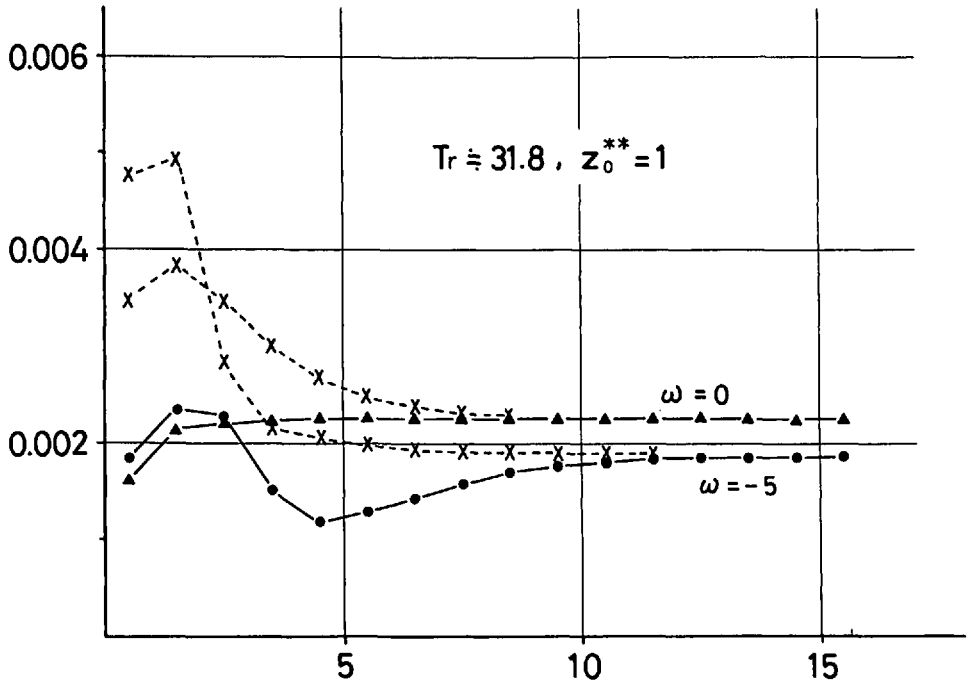

Figure 12. Variations with tidal period of the averaged dispersion coefficient in a linear profile current.

same reason as why the dispersion coefficient of particles with large settling velocity ($\omega^* < -1$) is smaller in the current with the Stokes layer.

4. Concluding remarks

In the basin with $T_r \ll 1$ (very shallow basin), which is beyond attention of this study, the current forms parabolic profile in the vertical, similar to Hagen- Poiseulle flow, because the viscosity is very large assuming $\nu_z = k_z$. Then the behavior during the initial stage might become out of the question since dispersion reaches the stationary stage rapidly in such a basin. At the stationary stage, particles are uniformly distributed in the vertical except for heavy particles like silt in such a basin (see Fig. 7). The boundary condition (2) does not represent such heavy particles. Dispersion of passive contaminant in a parabolic profile flow is almost analogous to the case of the linear profile flow (Fukuoka, 1973).

In the actual basin, which is generally expected to have large T_r, the current forms thin boundary layers because ν_z as well as k_z is small. It could be more reasonable in this case to introduce a current with a boundary layer than a current with linear profile assumed by many researchers in analysis of dispersion in oscillatory currents. A Stokes

layer can produce more effective dispersion on settling particles than on passive matter which has been already shown to be dispersed well by the layer (Yasuda, 1982, 1988).

This study, showing that existence of dispersing matter around the shear region induces effective dispersion in a current with nonuniform shear, suggests the possibility of dispersion of light particles drifting at the upper layer due to surface-layer flow generated by wind stress and dispersion of neutral particles drifting around the interface of water density due to internal wave. Such a situation could be observed in the field in other cases. These will be solved sequentially in the near future.

Although a current with Stokes layer is probably more realistic than a current with linear profile, the bottom layer of the real sea is a generation region of turbulence and is rather complicated not only physically but also chemically and biologically. In order to understand the real dispersion behavior of suspended particles, several problems still remain.

Acknowledgments. The work reported here was carried out as a part of the research conducted at the Government of Industrial Research Institute, Chugoku, and funded through the Environmental Protection Agency of the Japanese Government.

APPENDIX

The characteristic time of vertical mixing in a basin with the depth H is expressed as:

$$T_c = \frac{H^2}{k_z}. \tag{A-1}$$

In an oscillatory current, the characteristic time ratio of vertical mixing to the tidal period, T, is written as

$$T_r = \frac{T_c}{T} = \frac{H^2}{k_z T} = \frac{H^{*2}}{\pi}\frac{\nu_z}{k_z} \tag{A-2}$$

where H^* is the nondimensionalized water depth divided by the characteristic thickness of a Stokes layer $\delta(=\beta^{-1})$. The characteristic time of vertical mixing inside a Stokes layer is expressed as

$$T_{bc} = \frac{\delta^2}{k_z} = \frac{2}{\sigma}\frac{\nu_z}{k_z}. \tag{A-3}$$

If we pay attention to the whole depth, the characteristic settling velocity of particles is written as

$$W = \frac{H}{T_c} = \frac{k_z}{H}. \tag{A-4}$$

The nondimensionalized settling velocity can be expressed as

$$\omega = \frac{wH}{k_z}. \tag{A-5}$$

If our attention is paid to the Stokes layer, the characteristic and the nondimensionalized settling velocities are, respectively, expressed as

$$W^* = \frac{\delta}{T_{\delta c}} = \frac{k_z}{\delta} \tag{A-6}$$

$$\omega^* = \frac{w\delta}{k_z} = \frac{\omega}{H^*}. \tag{A-7}$$

In the usual analysis of the longitudinal dispersion, where the diffusing substance is well-mixed vertically, the depth H is an important characteristic scale in the dispersion. In the new analysis of the longitudinal dispersion of passive contaminant during the initial stage (Yasuda, 1988) and that of settling particles, the diffusing matter does not feel the finiteness of the depth and thus a Stokes layer could be a more important factor than the depth as a characteristic vertical scale.

REFERENCES

Aris, R. 1956. On the dispersion of a solute in a fluid flowing through a tube. Proc. Roy. Soc. London, *A235*, 67–77.

Awaya, Y. and K. Fujisaki. 1981. Mean velocity and longitudinal dispersion coefficient of heavy particles in open channel flow. Proc. Japan Soc. Civil Eng., *311*, 71–79 (in Japanese).

Bowden, K. F. 1965. Horizontal mixing in the sea due to a shearing current. J. Fluid Mech., *21*, 83–95.

Farlow, S. J. 1982. Partial Differential Equations for Scientists and Engineers. John Wiley & Sons Inc., NY, 402 pp.

Fischer, H. B. 1976. Mixing and dispersion in estuaries. Ann. Rev. Fluid Mech., *8*, 107–133.

Fischer, H. B., E. J. List, R. C. Y. Koh, J. Imberger and N. H. Brooks. 1979. Mixing in Inland and Coastal Water. Academic Press, NY, 483 pp.

Fukuoka, S. 1973. Longitudinal dispersion of matter in alternating shear flow. Research Bulletin C8, Dept. of Engineering, James Cook Univ. of North Queensland.

Holley, E. R., D. R. F. Harleman and H. B. Fischer. 1970. Dispersion in homogeneous estuary flow. J. Hydraul. Div. ASCE, *96*, 1691–1709.

Lamb, H. 1932. Hydrodynamics. 6th ed., Cambridge Univ. Press, Cambridge, 738 pp.

Okubo, A. 1967. The effect of shear in an oscillatory current on horizontal diffusion from an instantaneous source. Int. J. Oceanogr. Limnol., *1*, 194–204.

Smith, R. 1982. Contaminant dispersion in oscillatory flows. J. Fluid Mech., *114*, 194–204.

—— 1983. The contraction of contaminant distribution in reversing flows. J. Fluid Mech., *129*, 137–151.

Sumer, B. M. 1974. Mean velocity and longitudinal dispersion of heavy particles in turbulent open-channel flow. J. Fluid Mech., *65*, 11–28.

—— 1977. Settling of solid particles in open-channel flow. J. Hyd. Div. Proc. ASCE, *103*, 1323–1338.

Taylor, G. I. 1953. Dispersion of soluble matter in solvent flowing slowly through a tube. Proc. Roy. Soc. London, *A219,* 186–203.

—— 1954. The dispersion of matter in turbulent flow through a pipe. Proc. Roy. Soc. London, *A223,* 446–468.

Wilson, R. E. and A. Okubo. 1978. Longitudinal dispersion in a partially mixed estuary. J. Mar. Res., *36,* 427–447.

Yasuda, H. 1982. Longitudinal dispersion due to the boundary layer in an oscillatory current: theoretical analysis in the case of an instantaneous line source. J. Oceanogr. Soc. Japan, *38,* 385–394.

—— 1984. Longitudinal dispersion of matter due to the shear effect of steady and oscillatory currents. J. Fluid Mech., *148,* 383–403.

—— 1988. Longitudinal dispersion of matter due to the Stokes layer: its time-dependence in the case of an instantaneous point-source. J. Oceanogr. Soc. Japan, *44,* (in press).

Young, W. R., P. B. Rhines and C. J. R. Garrett. 1982. Shear-flow dispersion, internal waves and horizontal mixing in the ocean. J. Phys. Oceanogr., *12,* 515–527.

Received: *26 April, 1988;* revised: *22 September, 1988.*